Applied Physics Letters

On the compatibility of porous surfaces with cryogenic vacuum in future high-energy particle accelerators

Cite as: Appl. Phys. Lett. **114**, 153103 (2019); https://doi.org/10.1063/1.5085754
Submitted: 14 December 2018 . Accepted: 31 March 2019 . Published Online: 15 April 2019

L. Spallino, M. Angelucci, R. Larciprete, and R. Cimino

Applied Physics Letters ARTICLE scitation.org/journal/apl

On the compatibility of porous surfaces with cryogenic vacuum in future high-energy particle accelerators

Cite as: Appl. Phys. Lett. **114**, 153103 (2019); doi: 10.1063/1.5085754
Submitted: 14 December 2018 · Accepted: 31 March 2019 ·
Published Online: 15 April 2019

L. Spallino,[1,a)] M. Angelucci,[1] R. Larciprete,[1,2] and R. Cimino[1,3]

AFFILIATIONS

[1]Laboratori Nazionali di Frascati (LNF)-INFN, I-00044 Frascati, Italy
[2]Istituto dei Sistemi Complessi-CNR, via dei Taurini 19, 00185 Roma, Italy
[3]CERN, CH-1211 Geneva 23, Switzerland

[a)]luisa.spallino@lnf.infn.it

ABSTRACT

Recently, pulsed laser processing of Cu samples has been demonstrated to produce rough surfaces whose structuring at the nanoscale ensures an impressive reduction of the secondary electron yield. This feature has an undoubted appealing for applications in future high energy particle accelerators. However, the effective application of such laser treated surfaces in this context requires a rigorous evaluation of their vacuum behavior, especially when used at cryogenic temperatures. To this aim, here, we compare thermal programmed desorption between 20 and 70 K by dosing Ar multilayers of different thicknesses on a laser treated copper substrate and on its flat counterpart. Our results highlight that the spongelike structural features confer to the laser treated sample's non-negligible effects due to the gas-substrate interaction. This results in a much vaster and higher desorption temperature range with respect to what is observed from the flat substrates. This evidence could render it very difficult to find temperature intervals for which detrimental vacuum transients could be avoided in the cryogenic beam pipes. On these bases, although the electron cloud mitigation efficiency has been settled, before definitely including porous surfaces in any cryogenic machine design, all the consequences of having a rough rather than a flat wall should be carefully evaluated.

Electron-cloud effects (ECEs) are a critical issue for all modern high-energy charged particle accelerators. As a consequence of the strong coupling between the positively charged particle beam and the cloud of low energy electrons, detrimental machine instabilities may occur.[1–7] An efficient ECEs mitigation strategy is nowadays considered as a top priority challenge for the commissioning of the High Luminosity-Large Hadron Collider (HL-LHC)[8,9] and for the proton-proton Future Circular Collider (FCC-hh).[10] An intense program to study the driving forces governing ECEs formation has been recently launched.[2,3,5,6,11] Together with this study and complementary to it, a series of solutions have been proposed to mitigate ECEs. One of the main parameters governing the possibility to initiate ECEs effects in accelerators is the capability of their vacuum components to produce secondary electrons when an electron impacts the wall.[2,5,12] The Secondary Electron Yield (SEY) is defined as the ratio of the number of electrons leaving the sample surface (I_{out}) to the number of incident electrons (I_p). Some ECEs mitigation strategies have the objective of reducing such SEY,[5,13–16] and surface geometrical modification has been proved to be quite effective for this purpose. Macroscopically grooved surfaces do reduce the SEY and hence ECEs,[14,17–21] but they may increase the machine impedance well above the available budget.[22] Therefore, this solution must be considered with great care. A second approach consists in rendering surfaces rough at a microscopic or even nanoscopic level. Recently, an engineering method based on laser ablation (LASE) has been proposed. LASE can modify the surface at the nanoscale. It ensures an impressive reduction of SEY down to values even less than 1, depending on the detailed process and substrate material.[23,24] Moreover, this technology can be easily implemented both *in situ* and for large scale production.[25] The appealing and advantageous results of laser processing have brought in a short time laser treated copper (LASE-Cu) surfaces to be proposed for use in future accelerator technology. LASE-Cu is a potential candidate for

mitigating ECEs expected to occur on the beam screen (BS) in the cold bore of the dipoles of HL-LHC[8,9] and FCC-hh.[10] However, before definitely including LASE-surfaces in the machine design, the consequences of having a rough rather than a flat wall in the cryogenic ultrahigh vacuum (UHV) should be carefully evaluated.

When accelerator vacuum components are at cryogenic temperature, even small and unavoidable temperature (T) fluctuations may cause undesirable vacuum transients. If T is low enough, residual gas molecules such as H_2, CO, CO_2, H_2O, and CH_4 may be adsorbed on the cryogenic walls. Any T increase may induce their desorption and an unwanted pressure increase.[26] Many are the physical reasons requiring a very low operating vacuum pressure in an accelerator ($p \sim 10^{-8}$–10^{-10} mbar) and are specific to it and to its *operandi* mode.[27,28] High p, even if only for a short time or in a small section of the accelerator, may indeed have significant detrimental effects on machine performances. Therefore, a cryogenic vacuum system should avoid vacuum transient and pressure excursions.[29,30] This is why the choice of the working T of the cryogenic components is of paramount importance for the machine performances. For this reason, the BS in the cold bore of LHC is efficiently working at T ∼ 20 K. For cost reasons and the available cooling budget, the cold bore of FCC-hh has been proposed to operate in a temperature range between 40 K and 60 K.[31] Even for the high luminosity upgraded sections of LHC, the possibility either to operate its BS at ∼20 K[9] or to increase T to 40–60 K is presently under study.[32] At these temperatures, indeed, the saturated vapor pressure curves of the residual gas species adsorbed on the BS flat surfaces[33] are compatible with the operational pressure range planned for these machines.[28]

In the complex adsorption/desorption process on metal surfaces, different contributions are known to arise.[34–36] One is due to the three-dimensional ice layers and is dominant in a multilayer coverage regime. In this regime, the desorption T is basically determined by the saturated vapor pressure curve.[33] In a lower coverage regime, close or less than a monolayer, the adatoms are in direct contact with the surface and will generally be more strongly bound to it. Submonolayer coverages in direct contact with a metallic surface will require an higher temperature to desorb. Also, defect sites can increase the adsorption energy of many adsorbates, thus leading to desorption contributions at higher T.[34–36]

In accelerators, residual gases physisorb on flat *technical* surfaces. Such surfaces have a limited number of surface defects and are anyway covered by a contamination layer. For those flat *technical* samples, the desorption properties are dominated by the multilayer gas properties. This could not be the case for strongly *modified* surfaces. In the case of any porous structure and, specifically, for laser treated samples, the nanostructure surface may trap more efficiently adatoms even in the presence of adsorbed contaminants. Shifts of desorption T at higher values with respect to the one foreseen by the saturated vapor pressure curve and a significant spread of desorption T have already been observed in various porous systems.[37–40]

At cryogenic temperature, if strongly morphologically *modified* surfaces are present in the vacuum system, the evaluation of the saturated vapor pressure curves may not be sufficient to assess the absence of vacuum transient during small temperature fluctuations. Therefore, it is mandatory to explore the behavior of adsorbates on the artificially roughed surfaces as a function of temperature.

Here, this issue is investigated for a general case, by determining the thermal desorption characteristics of Ar dosed on a representative substrate of the LASE-Cu family. Ar has been chosen since its vapor pressure curve covers the p-T region of interest for the HL-LHC and FCC-hh operation conditions.[33] Ar is anyway a representative of a more general behavior we observe to occur also in the case of other gasses. The present study may be of relevance also for a vast number of applications, going from plasma physics[19,21] to satellite space-charge and radio-frequency break down,[18] where surface nanostructuring to reduce SEY is also being considered.

Experiments were performed at the Material Science Laboratory of the LNF-INFN (Frascati, Italy) in a UHV chamber, having a base pressure of $p < 2 \times 10^{-10}$ mbar and equipped with an He cooled cryogenic manipulator at the end of which we can insert, in the UHV condition, the sample under study which remains electrically insulated. The sample temperature can be varied and PID stabilized (within less than 0.2 K) in the 15–400 K range using a resistive heater controlled by a diode. Such a heater and a diode are placed on the grounded sample holder. Gas was delivered on the substrate held at 15–18 K by a gas dosing tube. This doser is built with chicanes so that the gas delivered onto the surface has a controlled speed and has an opening as big as the samples under study. It can be reproducibly inserted very close (<1 mm) to the sample surface, to reduce the dose seen by other cold surfaces or retracted away from it. In the retracted position, we can confidently assume that the amount of gas seen by the sample is the same as the one measured using the pressure gauge and mass spectrometer. The gas was dosed through a leak valve at a pressure of $p \sim 1.2 \times 10^{-9}$ mbar. The dosing units are given in Langumir (1 L = 1.33×10^{-6} mbar s). A 1 L dose (performed with the retracted doser) on the flat polycrystalline surface can be approximately assumed to be 1 monolayer (ML). This conversion is obtained by considering a mean density of Cu atoms on a polycrystalline surfaces lacking crystalline order and assuming an Ar sticking coefficient close to 1.[41] This equivalence has been used when calibrating the coverage on the flat sample by using SEY. LASE-Cu has an actual surface available for sticking Ar significantly larger than its sample geometrical surface. Therefore, the thickness of an Ar layer could be different on the porous and on the flat substrates even for nominally equal doses. Moreover, the assumption that the Ar pressure seen by the flat surface is homogeneous in all the porous fractals of the LASE-Cu cannot be considered to be valid. Therefore, the number of atoms deposited onto the LASE-Cu may depend on the actual sample nanostructure. Since the goal of this letter is to compare the behavior of LASE and flat Cu, we use a common variable for both cases, and since a ML on LASE-Cu is ill-defined, Langmuir units are used. The set-up is capable of measuring SEY to characterize the coverage of the Ar/poly-Cu surface. Experimental details about the SEY measurements are reported elsewhere.[2,5,11,42] SEY is known to be very sensitive to the presence of any overlayer,[43] and, more specifically, it depends on the actual Ar thickness.[5,43,44] Desorption was studied as a function of T, performing Thermal Programmed Desorption (TPD) measurements by using a quadrupole mass spectrometer (Hiden, HAL 3F PIC) while heating the sample with a rate of 0.005 K/s. Two categories of Cu substrates of 8×8 mm^2 were used: the flat Cu substrate and a representative sample of the LASE-Cu materials. The flat substrate is polycrystalline Cu (poly-Cu) with surface roughness less than 20 nm, as estimated by AFM measurements. Its cleanliness was addressed by SEY.[43] The

multilayer TPD results coming from it are anyway independent of the surface cleanliness. The LASE-Cu consists of copper colaminated stainless steel, the surface of which has been engineered by the pulsed laser ablation technique.[23]

Figure 1 shows the Scanning Electron Microscopy (SEM) images of the LASE-Cu sample, acquired with different magnifications using a SNE-3200M Tabletop SEM. In accordance with previous studies,[23–25] LASE-Cu surface topography is characterized by an inhomogeneous coral-like structure made of agglomerated nanoparticles forming a submicrometric highly porous network.

Three increasing Ar doses were considered, namely, 10, 25, and 100 L. We used such high doses so that, on the flat sample, we are in the multilayer regime. This is the coverage typically expected to occur in long exposures to residual gasses in an accelerator cryogenic environment.[29]

Figure 2 shows the SEY curves acquired as a function of Ar dosed from far on the poly-Cu sample and are in good agreement with literature results.[44] It is evident from Fig. 2 how sensitive is SEY to variations in Ar coverages, showing the effectiveness of using this simple spectroscopy as a technique capable of estimating them. By doing so, we can precisely (±10%) estimate the effective dose seen by the samples when dosing close to its surface even if, in the latter case, the pressure measured by the gauge and quadrupole is not representative of the Ar pressure seen by the surface. We could then set the dose parameters to be able to study the three aforementioned Ar doses also for the TPD experiments. SEY measurements on the Ar multilayer on the poly-Cu sample performed during TPD were also used for the sample temperature calibration. This was done for different gasses whose desorption temperature is in the T range that we are interested in. Below the T at which a certain gas multilayer desorption takes place, SEY is indeed one of the thick multilayers; just above this temperature, the measured SEY is the one of clean poly-Cu. Those transition temperatures, at which the gas multilayer desorbs from the surface,[33,45–47] have been used to calibrate the T read on the manipulator diode against the real surface temperature.

In Fig. 3, the TPD results are shown. The desorption curves observed from Ar dosed on the flat poly-Cu sample [Fig. 3(a)] show a sharp peak at T ∼28–30 K, having a Full Width at Half Maximum (FWHM) of ∼4 K. Above this peak, a ∼10, 25, 100 times smaller

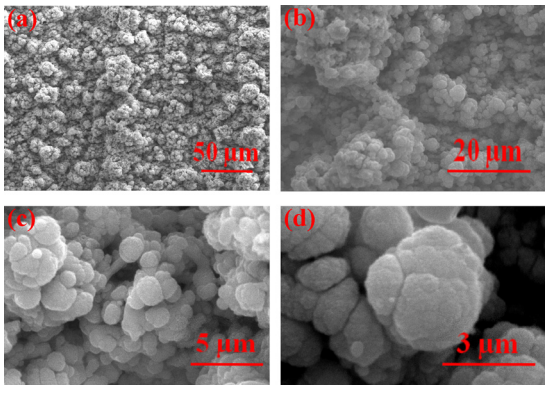

FIG. 1. SEM micrographs acquired with different magnifications of the LASE sample under investigation.

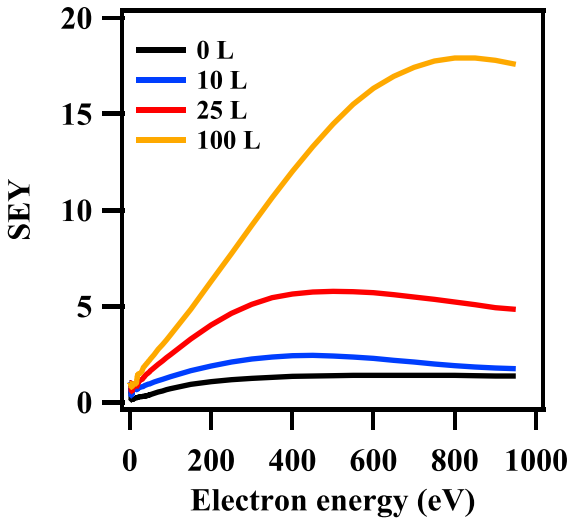

FIG. 2. SEY curves on varying the Ar exposure of the poly-Cu sample. The 0 L dose corresponds to the SEY of the bare poly-Cu sample.

signal is expected to appear due to the desorption of the first monolayer.[46,47] At present, our set-up does not allow us to observe it since not only it is too small but also probably hidden below the manipulator background signal which has been set to zero. As said before, the investigation of the monolayer/submonolayer regime is out of the scope of the present work. The data shown in Fig. 3(a) for the flat poly-Cu are in agreement with previous literature findings.[46–48] This single peak corresponds to the desorption of a condensed thick Ar layer. Its temperature is determined by the weak Ar-Ar van der Waals interaction energies.[33,45] In the inset of Fig. 3(a), we show the integral of the desorption peak. For the flat samples, the area under the sharp desorption peak linearly increases with the Ar dose, confirming that, in the studied coverage range, the sticking coefficient remain reasonably constant.

The desorption curves measured on the Ar dosed LASE-Cu surface [Fig. 3(b)] are characterized by broad profiles, whose peak temperatures and widths depend on the Ar dose. On increasing the Ar coverage by dosing 10, 25, and 100 L, the almost bell-shaped curves are centered at T ∼ 56 K, T ∼ 52 K, and T ∼ 50 K and have FWHM values of about 15, 20, and 25 K, respectively. Moreover, after 25 and 100 L, the Ar desorption at T ∼ 28–30 K is also observed. As reported in the inset, the area under the curve does not increase linearly on increasing the Ar dose. While there is not a final explanation to this observation, it could be an intrinsic feature of the porous nature of the sample that requires further study.

The marked differences in the Ar desorption behavior between the flat and the LASE surfaces clearly point out to the significant dependence of the process on the surface morphology. As already shown in Fig. 1, the laser treatment results in the formation of submicrometric and nanometric pores. Such micro- and nanostructuring, on the one hand, dramatically increases the specific surface, making the area accessible to atomic/molecular species much larger than the one available in the flat sample. On the other hand, the resulting nanostructured morphology determines a local increase in the adsorption energy for the Ar atoms in correspondence of under-coordinated sites

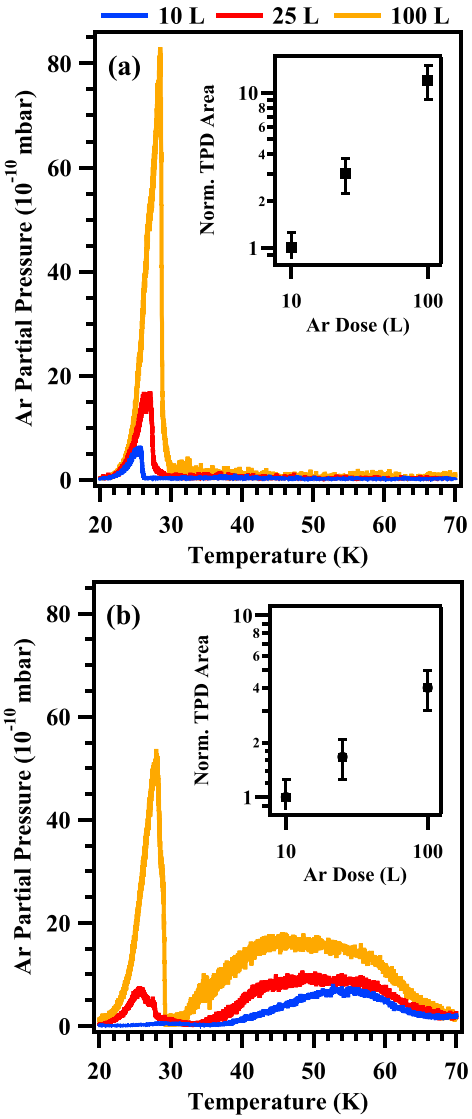

FIG. 3. TPD curves obtained monitoring the desorption of 10 L, 25 L, and 100 L of Ar dosed on the flat Cu substrate (a) and on a LASE-Cu sample (b). For each case, the inset shows the area under the curves as a function of Ar dose. The areas are normalized to the value recorded at the lower dose.

and defects.[35,36,49] The desorption of the Ar atoms close to defected surfaces and/or trapped in the pores of the LASE-Cu surface is shifted to higher temperature. In contrast, multilayer Ar atoms, which basically feel only the Ar-Ar forces, desorb around 28–30 K, as in the case of the flat sample. The broadening of the high temperature TPD component measured for the LASE-Cu samples cannot be attributed to the spread of the adsorption energies only but, following the pore geometry limited desorption model,[38] a contribution in this sense might also derive from multiple desorption-re-adsorption cycles in the inner submicrometric pore. The progressive occupation of all available adsorption sites (pores wall included) could explain the gradual broadening of the TPD peak above 30 K observed with increasing Ar dose.

This investigation serves as a proof of principle to address the vacuum compatibility of LASE-Cu when used at cryogenic temperature in high-energy particle accelerators. More in general, the data here presented call for additional careful studies to validate the use in cryogenic vacuum of all very rough or porous surfaces. In this contest, even the growth mode of the amorphous carbon (a-C) coating proposed for the base-line design of HL-LHC[9] must be studied and optimized in light of the present results. In fact, it is known that, depending on the actual mode and mechanisms used to grow the a-C film, it can be produced nearly as rough as the LASE.[32] Although all these porous materials are intrinsically optimal e^--cloud suppressors, troubling consequences could arise from their exploitation in a UHV environment at cryogenic temperature. Their gas desorption may spread over a broader than expected temperature range. From the point of view of their vacuum behavior, this could render very difficult to find temperature intervals where vacuum transients can be excluded to occur for all the molecular species composing the residual gas in the accelerator.

Conceptually identical data have been obtained by dosing the two different Cu surfaces with CO and CH_4. These gasses are expected to be part of the residual gas composition of any accelerator vacuum system. For these gasses, when measuring TPD from a flat surface, we observe a sharp peak (with a FWHM $\sim$ 4 K). Such a TPD signal increases on increasing gas doses and occurs at the specific desorption T characteristic of the dosed gas layer.[33] When dosing on LASE-surfaces, an identical behavior as the one shown in Fig. 3(b) is observed. The TPD curves measured from CO and CH_4 on the LASE-Cu surface are characterized by the same presence of the additional broad component, as observed and discussed for the Ar case. This confirms that what has been here presented to occur for Ar deposition on porous materials does not depend on the Ar gas properties but depends on the micro-nanostructure of the substrate. The observed behavior has to be expected to occur for all cryosorbed gasses.

In conclusion, while the use and optimization of LASE and of all porous surfaces to mitigate SEY is quite advanced, a significant additional experimental campaign is necessary to validate their use in future accelerators. Given the present understanding, their vacuum behavior need to be carefully studied and confirmed to be compliant with the usually very stringent vacuum requirements of most cryogenic accelerators. Moreover, it is worth noting that non-thermal mechanisms are also acknowledged to markedly contribute to accelerator vacuum behavior. Dynamic processes, such as ions, electrons, and photons stimulated desorption,[50] will always occur during accelerator's performance. The investigation of these effects is then mandatory to completely assess the validity of LASE and, more in general, of any porous surfaces in accelerators.

This work was supported by *The European Circular Energy-Frontier Collider Study* (EuroCirCol) project (Grant No. 654305) and by the MICA project funded by INFN Scientific National Committee 5. We thank V. Baglin, P. Chiggiato, R. Kersevan, O. Malyshev, and R. Valizadeh for useful discussions and for the LASE samples and the DAΦNE-L team for technical assistance.

REFERENCES

[1]G. Rumolo, A. Z. Ghalam, T. Katsouleas, C. K. Huang, V. K. Decyk, C. Ren, W. B. Mori, F. Zimmermann, and F. Ruggiero, Phys. Rev. Spec. Top.-Accel. Beams **6**, 081002 (2003).

[2]R. Cimino, I. Collins, M. Furman, M. Pivi, F. Ruggiero, G. Rumolo, and F. Zimmermann, Phys. Rev. Lett. **93**, 014801 (2004).
[3]F. Zimmermann, Phys. Rev. Spec. Top.-Accel. Beams **7**, 124801 (2004).
[4]*ECLOUD'12: Joint INFN-CERN-EuCARD-AccNet Workshop on Electron-Cloud Effects, CERN Yellow Reports: Conference Proceedings*, edited by R. Cimino, G. Rumolo, and F. Zimmermann (CERN, Geneva, 2013).
[5]R. Cimino and T. Demma, Int. J. Mod. Phys. A **29**, 1430023 (2014).
[6]G. Rumolo and G. Iadarola, in *CERN Yellow Reports: School Proceedings* (2017), Vol. 3, p. 411.
[7]K. Ohmi, F. Zimmermann, L. Mether, and D. Schulte, "Study of electron cloud instabilities in fcc-hh," Technical Report CERN-ACC-2015-285 (2015).
[8]See http://hilumilhc.web.cern.ch/ for for details on the project.
[9]G. Apollinari, I. B. Alonso, O. Brüning, P. Fessia, M. Lamont, L. Rossi, and L. Tavian, *High-Luminosity Large Hadron Collider (HL-LHC): Technical Design Report* (CERN, 2017).
[10]See http://fcc.web.cern.ch/ for details on the project.
[11]R. Cimino, M. Commisso, D. R. Grosso, T. Demma, V. Baglin, R. Flammini, and R. Larciprete, Phys. Rev. Lett. **109**, 064801 (2012).
[12]M. Furman and M. Pivi, Phys. Rev. Spec. Top.-Accel. Beam **5**, 124404 (2002).
[13]Y. Suetsugu, K. Kanazawa, K. Shibata, and H. Hisamatsu, Nucl. Instrum. Methods Phys. Res., A **556**, 399 (2006).
[14]M. Pivi, F. King, R. Kirby, T. Raubenheimer, G. Stupakov, and F. Le Pimpec, J. Appl. Phys. **104**, 104904 (2008).
[15]Y. Suetsugu, H. Fukuma, L. Wang, M. Pivi, A. Morishige, Y. Suzuki, M. Tsukamoto, and M. Tsuchiya, Nucl. Instrum. Methods Phys. Res., A **598**, 372 (2009).
[16]C. Yin Vallgren, G. Arduini, J. Bauche, S. Calatroni, P. Chiggiato, K. Cornelis, P. C. Pinto, B. Henrist, E. Métral, H. Neupert, G. Rumolo, E. Shaposhnikova, and M. Taborelli, Phys. Rev. Spec. Top.-Accel. Beams **14**, 071001 (2011).
[17]A. Krasnov, Vacuum **73**, 195 (2004).
[18]V. Nistor, L. A. González, L. Aguilera, I. Montero, L. Galán, U. Wochner, and D. Raboso, Appl. Surf. Sci. **315**, 445 (2014).
[19]C. Swanson and I. D. Kaganovich, J. Appl. Phys. **120**, 213302 (2016).
[20]M. Ye, D. Wang, and Y. He, J. Appl. Phys. **121**, 124901 (2017).
[21]C. Swanson and I. D. Kaganovich, J. Appl. Phys. **122**, 043301 (2017).
[22]*ICFA Mini-Workshop on Impedances and Beam Instabilities, CERN Yellow Reports: Conference Proceedings*, edited by V. Brancolini, G. Rumolo, M. R. Masullo, and S. Petracca (CERN, Geneva, 2018).
[23]R. Valizadeh, O. B. Malyshev, S. Wang, S. A. Zolotovskaya, W. Allan Gillespie, and A. Abdolvand, Appl. Phys. Lett. **105**, 231605 (2014).
[24]R. Valizadeh, O. Malyshev, S. Wang, T. Sian, M. D. Cropper, and N. Sykes, Appl. Surf. Sci. **404**, 370 (2017).
[25]S. Calatroni, E. G.-T. Valdivieso, H. Neupert, V. Nistor, A. T. P. Fontenla, M. Taborelli, P. Chiggiato, O. Malyshev, R. Valizadeh, S. Wackerow *et al.*, Phys. Rev. Accel. Beams **20**, 113201 (2017).
[26]C. Benvenuti, J. Cazeneuve, P. Chiggiato, F. Cicoira, A. E. Santana, V. Johanek, V. Ruzinov, and J. Fraxedas, Vacuum **53**, 219 (1999).
[27]O. Gröbner, Vacuum **60**, 25 (2001).
[28]V. Baglin, L. Tavian, P. Lebrun, and R. van Weelderen, "Cryogenic beam screens for high-energy particle accelerators," Technical Report CERN-ATS-2013-006 (2013).
[29]V. Baglin, "Vacuum transients during LHC operation," in *1st LHC Project Workshop*, Chamonix, France, 19–23 January (2004), p. 275.
[30]W. C. Turner, J. Vac. Sci. Technol., A **14**, 2026 (1996).
[31]F. J. P. Rodriguez, P. Chiggiato, C. Garion, J. F. Topham, and on behalf of EuroCirCol WP4, "Preliminary beam screen and beam pipe engineering design: Deliverable D4.3," Technical Report No. CERN-ACC-2019-0023 (CERN, Geneva, 2017).
[32]R. Salemme, V. Baglin, G. Bregliozzi, and P. Chiggiato, in *Proceeding of the International Particle Accelerator Conference (IPAC'16)*, Busan, Korea, 8–13 May 2016, International Particle Accelerator Conference No. 7 (JACoW, Geneva, Switzerland, 2016), p. 3663.
[33]R. E. Honig and H. O. Hook, RCA Rev. **21**, 360 (1960).
[34]R. Brosseau, M. Brustein, and T. Ellis, Surf. Sci. **294**, 243 (1993).
[35]J.-Y. Park, S.-J. Kahng, U. Ham, Y. Kuk, K. Miyake, K. Hata, and H. Shigekawa, Phys. Rev. B **60**, 16934 (1999).
[36]L. Baker, B. Holsclaw, A. E. Baber, H. L. Tierney, E. C. H. Sykes, and A. J. Gellman, J. Phys. Chem. C **114**, 18566 (2010).
[37]J. Thrower, M. Collings, F. Rutten, and M. McCoustra, Mon. Not. R. Astron. Soc. **394**, 1510 (2009).
[38]A. Paldor, G. Toker, Y. Lilach, and M. Asscher, Phys. Chem. Chem. Phys. **12**, 6774 (2010).
[39]A. Clemens, L. Hellberg, H. Grönbeck, and D. Chakarov, Phys. Chem. Chem. Phys. **15**, 20456 (2013).
[40]T. Suhasaria, J. Thrower, and H. Zacharias, Mon. Not. R. Astron. Soc. **472**, 389–399 (2017).
[41]L. L. Levenson, J. Vac. Sci. Technol. **8**, 629 (1971).
[42]R. Larciprete, D. R. Grosso, M. Commisso, R. Flammini, and R. Cimino, Phys. Rev. Spec. Top.-Accel. Beams **16**, 011002 (2013).
[43]L. Gonzalez, M. Angelucci, R. Larciprete, and R. Cimino, AIP Adv. **7**, 115203 (2017).
[44]J. Cazaux, Y. Bozhko, and N. Hilleret, Phys. Rev. B **71**, 035419 (2005).
[45]A. Ferreira and L. Lobo, J. Chem. Thermodyn. **40**, 1621 (2008).
[46]W. Berthold, P. Feulner, and U. Höfer, Chem. Phys. Lett. **358**, 502 (2002).
[47]A. Damm, K. Schubert, J. Güdde, and U. Höfer, Phys. Rev. B **80**, 205425 (2009).
[48]M. Stichler, P. Zebisch, M. Weinelt, and H.-P. Steinrück, Surf. Sci. **348**, 370 (1996).
[49]P. Ayotte, R. S. Smith, K. P. Stevenson, Z. Dohnálek, G. A. Kimmel, and B. D. Kay, J. Geophys. Res. Planets **106**, 33387 (2001).
[50]G. Bregliozzi, G. Lanza, V. Baglin, and J. Jimenez, Vacuum **86**, 1682 (2012).